The effects of sampling resolution on the surface albedos of dominant land cover types in the North American boreal region

Andrew Davidson[1 2 3] & Shusen Wang[2]

[1] Noetix Research Inc.

265 Carling Avenue, Suite 403

Ottawa, Ontario

Canada K2S 2E1

[2] Environmental Monitoring Section,

Applications Division,

Canada Centre for Remote Sensing,

588 Booth Street,

Ottawa, Ontario

Canada K1A 0Y7

[3] Author to whom correspondence should be sent.

Email: (E-mail: Andrew.Davidson@CCRS.NRCan.gc.ca).

Tel: (613) 943 8825

Fax: (613) 947 1406

Abstract

The central role that land surface albedo (α) plays in the physical climate system makes it a key component of climate and ecosystem models. However, this parameter remains one of the largest radiative uncertainties associated with modeling attempts. Uncertainty occurs because models commonly prescribe albedo using *in situ* observations, which are rarely sufficiently dense to accurately characterize albedo at a regional scale. This is especially problematic over seasonally snow-covered landscapes such as the boreal forest. The aims of this study are to (a) analyze and compare the local- and regional-scale albedo characteristics of the dominant land cover types found within the North American boreal region, (b) assess the the effects of snow cover on these patterns, and (c) quantify the potential bias that can result from using local-scale observations to describe surface albedos across larger geographical extents. Our study is based on local-scale *in situ* observations and regional-scale satellite (GOES) measurements that were collected as part of the Boreal Ecosystem-Atmosphere Study (BOREAS). Our results show (a) that the albedo patterns among land cover types are generally consistent at local and regional scales, (b) that snow cover not only increases the albedo of all cover types, but also their sensitivities to changes in solar zenith angle, and (c) that weekly-averaged *in situ* observations provide a reasonable characterization of regional-scale albedo when under snow-free conditions, but a poor characterization when snow is present. Land cover albedo characteristics are caused by canopy properties that influence within-canopy shadowing. The disparity between *in situ* albedo observations and those collected over low-density needleleaf forest are particularly a concern because this cover type comprises a significant proportion of the boreal region, and its mis-specification in climate models could lead to large errors in energy balance. Further studies should focus on reducing the disparity between albedo datasets over snow-covered surfaces. They should also consider the effects of diffuse radiation, as well as finer time scales, on the above relationships.

0. Introduction

Land surface albedo – the fraction of incident (shortwave) solar radiation reflected in all directions by the land surface (Pinty and Verstraete, 1992) – is one of the most important parameters controlling the earth's climate. Albedo is important because it directly determines the amount of solar energy absorbed by the ground, and hence, the amount of energy available for heating the ground and lower atmosphere and evaporating water (Rowe, 1991). It also affects the global climate system indirectly by controlling the ecosystem energy, water and carbon processes that regulate greenhouse gas exchange (Wang et al., 2002). A detailed knowledge of how albedo changes through space and time is crucial to understanding the global radiation balance and its influence on climate and vegetation dynamics (Henderson-Sellers and Wilson, 1983; Lucht et al., 2000b).

The central role that surface albedo plays in the physical climate system makes it a key component of general circulation models (GCMs). For example, model simulations by Betts (2000) found that changes in albedo brought about by the reforestation of boreal forest can offset the negative radiative forcing that is expected from carbon sequestration. The accurate parameterization of albedo in models is crucial because its mis-specification usually leads to large errors in modelled radiation balances (Betts and Ball, 1997). Unfortunately, however, surface albedo remains one of the largest radiative uncertainties associated with modeling attempts (IPCC, 2001; Liang et al., 2002a). Uncertainty occurs because albedo is only crudely represented in GCMs. GCMs commonly prescribe albedo by associating broad land cover classes with a set of "typical" albedo values derived from *in situ* observations (Li and Garand, 1994). These observations, which are collected at much finer spatial resolutions (< 100m) than those utilized by GCMs (1º or coarser), are rarely able to accurately characterize the grid- and sub-grid-scale spatio-temporal variations in albedo required by climate models (Li and Garand, 1994; Gu and Smith, 1997; Gu et al., 1997; Song and Gao, 1999; Liang et al., 2002b). The effects of this scale mismatch need to be better understood if *in situ* albedo measurements are to be "scaled up" to the resolutions needed for climate modelling studies. The explicit consideration of

scale is important because scale-dependence is an inherent property of geographical phenomena (Cao and Siu-Ngan Lam, 1997), and albedo-related processes that appear important at small scales may be unimportant at coarser scales. These scaling effects are particularly a concern over heterogeneous environments whose surface albedos vary dramatically through both space and time.

The seasonally snow covered landscape of the boreal forest is one such environment. This ecosystem, which covers 8% of the earth's land surface (Bonan et al., 1992), comprises the contiguous green belt of conifer and deciduous trees that encircle the earth at latitudes greater than 48° N. The surface albedo properties of this vast ecosystem have a huge influence on the climate of the northern hemisphere and the global carbon cycle. This makes the boreal forest an important biome to represent correctly in GCMs (Sellers et al., 1997). However, the possibility of snow cover makes the albedo of boreal forest highly variable through space and time (Jin et al., 2002). Thus, this parameter is often difficult to accurately specify in climate models. Of particular interest to modellers is a greater understanding of how snow cover affects albedo at local, regional and global scales (Vikhamar and Solberg, 2003).

The general aims of this study are to (a) analyze and compare the local- and regional-scale albedo characteristics of the dominant land cover types found within the North American boreal region, (b) assess the the effects of snow cover on these characteristics, and (c) quantify the potential bias that can result from using local-scale observations to describe surface albedos across larger geographical extents. Our study is based on local-scale *in situ* observations and regional-scale satellite (GOES) measurements that were collected as part of the Boreal Ecosystem-Atmosphere Study (BOREAS) (Newcomer et al., 2000; Nickeson et al., 2002). Because of the uncertainty associated with GOES-derived albedo observations under cloudy sky, we focus our analysis only on albedo collected under clear-sky conditions.

1. Methods

1.1 Study Region

The study region focuses on a 1000 x 1000 km region of the North American boreal forest. This region encompasses most of the Canadian Provinces of Alberta and

Saskatchewan, and contains a variety of land cover types whose distributions are strongly controlled by temperature and moisture availability. The south-western portion of the study area is dominated by a mosaic of natural grassland and cropland. The north-eastern portion of the study area is dominated by barren landscapes containing shrubs and/or lichens. Forest, burned land and bodies of water dominate the landscape between these extremes. Forested land is predominantly mixed (broadleaf/needleleaf) in the south of the region, and needleleaf of varying density in the north.

1.2 Local-Scale Data

2.2.1 Tower-Derived Surface Radiation Data

Local-scale radiation data (<1km^2) were collected using tower-mounted radiation sensors at 10 separate locations within the study region between January 1st and December 31st 1996 (Newcomer et al., 2000; Shewchuk, 2000). Two sites were located over grassland, one was located over Old Aspen, four were located over mixed spruce and poplar stands, and the remaining three were located over Jackpine. We use data from 7 of the sites in this paper. These are (a) the grassland sites located at Meadow Lake (54° 07' 28" N, 108° 31' 21" W) and Saskatoon (52° 09' 50" N, 106° 36' 12" W), (b) the Old Aspen-dominated site (SSA-OA) located in the BOREAS Southern Study Area (53° 37' 45" N, 106° 11' 51" W), (c) the Spruce- and Poplar-dominated site near La Ronge (55° 07' 31" N, 105° 17' 35" W), and (d) the old Jackpine-dominated sites located in the Southern Study Area (SSA-OJP; 54° 54' 59" N, 104° 41' 26" W), the Northern Study Area (NSA-OJP; 55° 55' 41" N, 98° 38' 26" W), and at Lynn Lake (56° 51' 50" N, 101° 05' 33" W). The Old Aspen site is a mostly pure strand of trembling Aspen (*Populus tremuloides* Michx.) about 70 years old, with a stand density of about 830 stems ha^{-1} (Yang et al., 1999). The Jackpine (*Pinus banksiana* Lamb.) sites ranged in age and stem density. The SSA-OJP site contained trees of 50-65 years old and had a stem density 1300-3500 stems ha^{-1}, while the NSA-OJP site contained trees of 60-75 years old and had a stem density of 1600-4000 stems ha^{-1} (Chen et al., 1997). Tree density data were unavailable for the Lynn Lake Jackpine site and the Spruce (*Picea mariana*) and Poplar (*Populus balsamifera*) dominated sites.

Radiation data were collected using automatic meteorological stations (AMS). Each AMS included a Rohn tower, on which sensors were mounted. These sensors included upward- and downward-looking pyranometers that recorded incoming and reflected shortwave radiation ($S\downarrow$ and $S\uparrow$ (in Wm^{-2}); λ = 0.285 to 2.800μm), and an upward-looking PAR Sensor that recorded incoming photosynthetically active radiation ($PAR\downarrow$ (in Wm^{-2}); λ = 0.4 to 0.7μm). Sensors were situated 2 to 6m above the canopy top, and were exposed to the weather at all times. $S\downarrow$, $S\uparrow$ and $PAR\downarrow$ measurements were recorded simultaneously at 5s intervals throughout the data collection period. Data loggers automatically generated 15-minute average values from these data. A detailed description of these sites, instrumentation used, siting and data quality assurance is provided by Shewchuk (2000).

We screened the time-averaged radiation observations for "suspect" data. Our particular concern was the identification of low and incorrect $S\downarrow$ values that might result from snow and ice build-up on the upward-looking pyranometer during winter. Our data screening followed the methods of Betts and Ball (1997), who rejected observations if their ratios of $S\downarrow$ and $PAR\downarrow$ differed from those expected under 'normal' sensor conditions (i.e. if $PAR\downarrow / S\downarrow > 0.6$). High albedo values that came close to meeting this criterion were also filtered out if they fell inside sequential days of bad data. Data screening generally eliminated observations of very low $S\downarrow$ (< 15 Wm^{-2}) in January and November / December.

We then identified pairs of $S\downarrow$ and $S\uparrow$ observations that were recorded under clear-sky (cloud-free) conditions. Clear-sky conditions were determined by the criterion $S\downarrow / (S_o \cos\phi) > 0.6$ (see Wang et al., 2002), where ϕ corresponds to the SZA (SZA) at the time and place of measurement (in radians; see Cornwall et al., (2003), and S_o corresponds to the solar constant (1367 Wm^{-2}). Clear-sky shortwave albedo, $\alpha = S\downarrow / S\uparrow$, was then calculated for each pair of clear-sky $S\downarrow$ and $S\uparrow$ observations. Lastly, we matched these observations with their corresponding snow cover values. The resulting data set contained approximately 6,500 albedo-SZA-snow observations for each tower site (≈ 46,000 observations in total).

2.2.2 Snow Data

Snow depth data were also collected automatically at each AMS in 1996. At each sampling location, snow depth was recorded (in mm) every 5s using a Snow Depth Gauge. Data loggers then automatically generated 15-minute average values from these data. Time-averaged snow-depth data were further processed to produce a continuous dataset for modelling purposes (Knapp and Newcomer, 1999; Newcomer et al., 2000). Missing snow cover data were filled by the linear interpolation of bounding values. We then reclassed these data as either "snow-present" (snow depth > 0) or "snow-absent" (snow depth = 0).

2.3 Regional-Scale Data

2.3.1. Satellite-Derived Surface Radiation Data

Regional-scale radiation data ($10^6 km^2$) were collected using the Geostationary Operational Environmental Satellite (GOES-8) (Smith et al., 2001). These data were acquired in five spectral bands (one visible, four infrared), and covered the study area at a spatial resolution of 4km. GOES-8 data collection commenced on February 13th 1996 (day-of-year 44) and ended on October 22nd 1996 (day-of-year 296). Spectral data were collected every 30 minutes when possible, providing a total data set of almost 3800 images. Fifteen or more images were collected for most days in the data collection period, although some dates were poorly sampled (n < 5). Further gaps appeared where image pixels were flagged as "missing". However, these values were mostly restricted to images acquired at large solar zenith angles (SZAs). We used GOES-8 observations because the geostationary orbit of this satellite allowed the continuous measurement of surface albedo, allowing regional-scale SZA-albedo relationships to be calculated at the same temporal resolution as the local-scale observations.

Smith et al., (2001) calibrated the visible-band image data then used it as input to a physical retrieval algorithm (Gu and Smith, 1997; Gu et al., 1997; Gu et al., 1999). This algorithm – which included several atmospheric corrections (Rayleigh scattering, water vapor and ozone absorption, aerosol and cloud attenuation) and a bi-directional reflectance correction for surface reflectance anisotropy – was used to extract various radiation parameters from the image data. These parameters, including the incoming

shortwave radiation at the ground surface ($S\downarrow$; λ = 0.3 μm – 3.0 μm) and surface shortwave albedo (α; λ = 0.3 μm – 3.0 μm), were calculated on a per-pixel basis for each of the visible-band images. Validations of the retrieval algorithm (Gu et al., 1999) showed only small biases in $S\downarrow$ and α against *in situ* measurements under clear-sky conditions. A detailed explanation of GOES data processing and validation, as well as the resulting dataset's errors and limitations, are provided elsewhere (Gu and Smith, 1997; Gu et al., 1997; Gu et al., 1999; Smith et al., 2001).

We isolated the albedo observations that were recorded under clear-sky conditions. This was achieved through the per-pixel application of the criterion described earlier ($S\downarrow / (S_o \cos\phi) > 0.6$; Section 2.1.1) to each of the GOES-8 $S\downarrow$ images. In this application of the criterion, $S\downarrow$ corresponded to the incoming shortwave radiation of each pixel (calculated by the physical retrieval algorithm), while ϕ corresponded to the SZA at the pixel's centre (Cornwall et al., 2003; the coordinates of each pixel's center in the GOES-8 imagery were provided as part of the GOES-8 data archive}. We then matched the radiation and SZA observations with their corresponding snow cover and cover values (see following sections). The resulting data set contained almost 19 million albedo-SZA-snow-cover observations.

2.3.2. Snow Data

We used the Northern Hemisphere EASE-grid Weekly Snow Cover and Sea Ice Extent Version 2 product (Armstrong and Brodzik, 2002) to map the spatial and temporal distribution of snow cover over the BOREAS region during 1996. This data set comprised weekly snow cover maps at a spatial resolution of 25km. Grid cells over the BOREAS region were either categorized as snow-free or snow-covered. However, the coarse spatial resolution of these data meant that it could not be used to accurately identify the snow cover status of GOES-8 pixels during times of the year where large sub-pixel variability in snow cover occurred. This is because albedo-cover relationships derived for snow-covered surfaces during these periods would also include albedos that corresponded to snow-free surfaces, and vice versa, resulting in large (and unknown) errors of omission and commission. As a result, we excluded these short periods – which

coincided with spring snowmelt and late fall snowfall – from our overall analysis. The entire weekly snow and ice data set (1966 through 2001) is available from the National Snow and Ice Data Center (http://www-nsidc.colorado.edu/data/nsidc-0046.html).

2.3.3. Land Cover Data

We used the 1995 1km-resolution digital land cover map of Canada (Cihlar et al., 1999) to map the spatial distribution of land cover types across the BOREAS region in 1996. We combined similar land cover classes in this 31-class data set to produce an 18-class land cover map. This map was then resampled to a spatial resolution of 4km using a modal resampling method. Resampling resulted in only a slight loss of information from the original 1km 18-class classification (the agreement between the land cover classes of pixels in the 1km 18-class land cover map and their corresponding locations on the 4km map was > 97%). We then identified "training areas" for each of the most dominant cover types in the 18-class classification. Training areas were located in relatively homogeneous (non-fragmented) regions of each land cover type. Information from these areas was used to derive the α-SZA-snow relationships presented in this study. This approach allowed land cover and GOES-8 albedo information to be compared at commensurable spatial resolutions. The trade-off between land cover accuracy and computer processing time was deemed reasonable for our purposes.

3. Results

3.1 Local-scale data

The overall tower-based relationships between albedo and cover type are illustrated in Figures 1(a) and (b). Where snow is present (Figure 1(a)), grassland canopies generally reflect more incident shortwave radiation than broadleaf forest canopies, broadleaf forest reflects more sunlight than needleleaf forest, and needleleaf forest is more reflective than mixed forest. A similar trend exists where snow is absent (Figure 1(b)). The albedos of snow-covered canopies are higher and more variable than those of snow-free canopies (compare means and error bars in Figure 1(a) with Figure 1(b)). This is particularly true for both grassland sites.

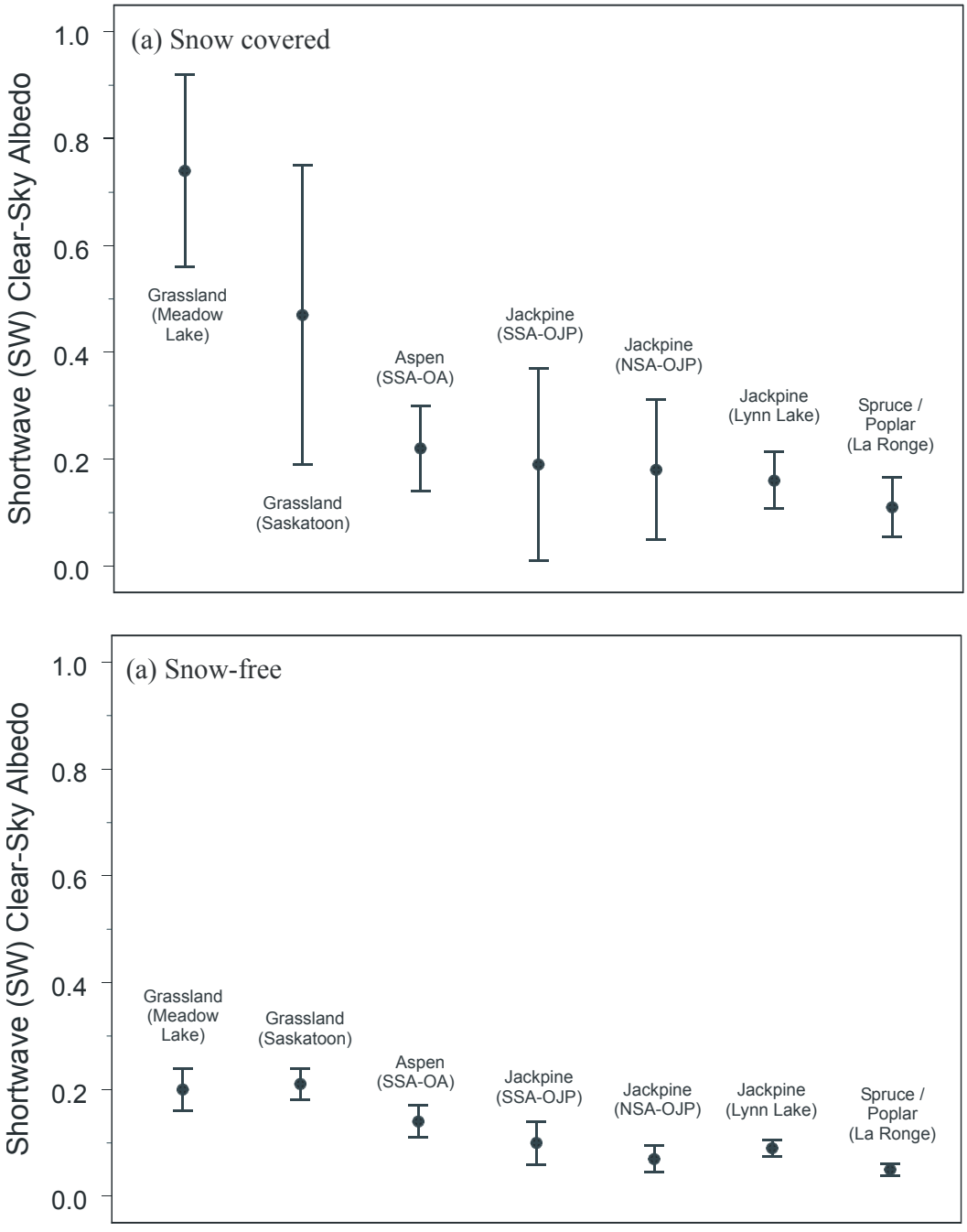

Figure 1. The relationship between land cover type and clear-sky albedo as derived from AMS measurements. Panels show the mean albedo of each vegetation type and its variability (standard deviation around mean) for surface conditions where snow is present (a) and absent (b).

Figure 2 shows the temporal variations in albedo for snow-covered and snow-free periods at six of the tower sites. This figure also shows the effects that solar zenith angle have on land surface albedo. Figure 2 reinforces the previously described differences in albedo between snow-covered and snow-free ground conditions (especially the large differences in snow/no-snow albedos for grassland sites). The influence of SZA on surface albedo varies with cover type and snow cover conditions. The effects of SZA on albedo are varied when snow is present. However, large effects of SZA on surface albedo are observed over grassland (Figures 2(a) and (b)) and broadleaf (Figure 2(c)) canopies when snow is absent. These effects are generally smallest at the beginning and end of the growing season, and largest near the middle of the growing season (e.g. Figure 2(c)). During snow-free periods, the effects of SZA on the albedos of needleleaf forest (Figures 2(d) and (e)) and mixed forests (Figure 2(f)) change little through time. The peaks in standard deviations from the mean albedos generally occur during transitions from snow-covered to snow-free periods (i.e. snowmelt) and vice versa (i.e. snowfall). These peaks reflect a high variability of albedo within each 5° range in SZA during these periods.

Figure 3 provides an example of the diurnal patterns of albedo for winter and summer days. Figure 3 shows that the diurnal effects of SZA on albedo vary with season and land cover type. These effects are large during the summer for grasslands and broadleaf forest (Figure 3(b)). The mixed forest and needleleaf forest sites show similar diurnal SZA-albedo relationships between seasons.

3.2 Regional-scale data

The overall regional-scale relationships between albedo and cover type are illustrated in Figures 4(a) and (b). The patterns of albedo among broadleaf forest, needleleaf forest and mixed forest canopies are generally consistent with those described for local-scale data. However, one notable exception to this general trend is the high albedo of low-density needleleaf forest when snow is present. The presence of snow affects the magnitudes of surface albedo, as well as their within-type variabilities. The presence of snow raises the albedo of canopies, especially those of low- (+ 0.33), medium- (+ 0.16) and high-density needleleaf forest (+ 0.19). Snow-covered canopies also show greater variations in albedo compared to snow-free canopies.

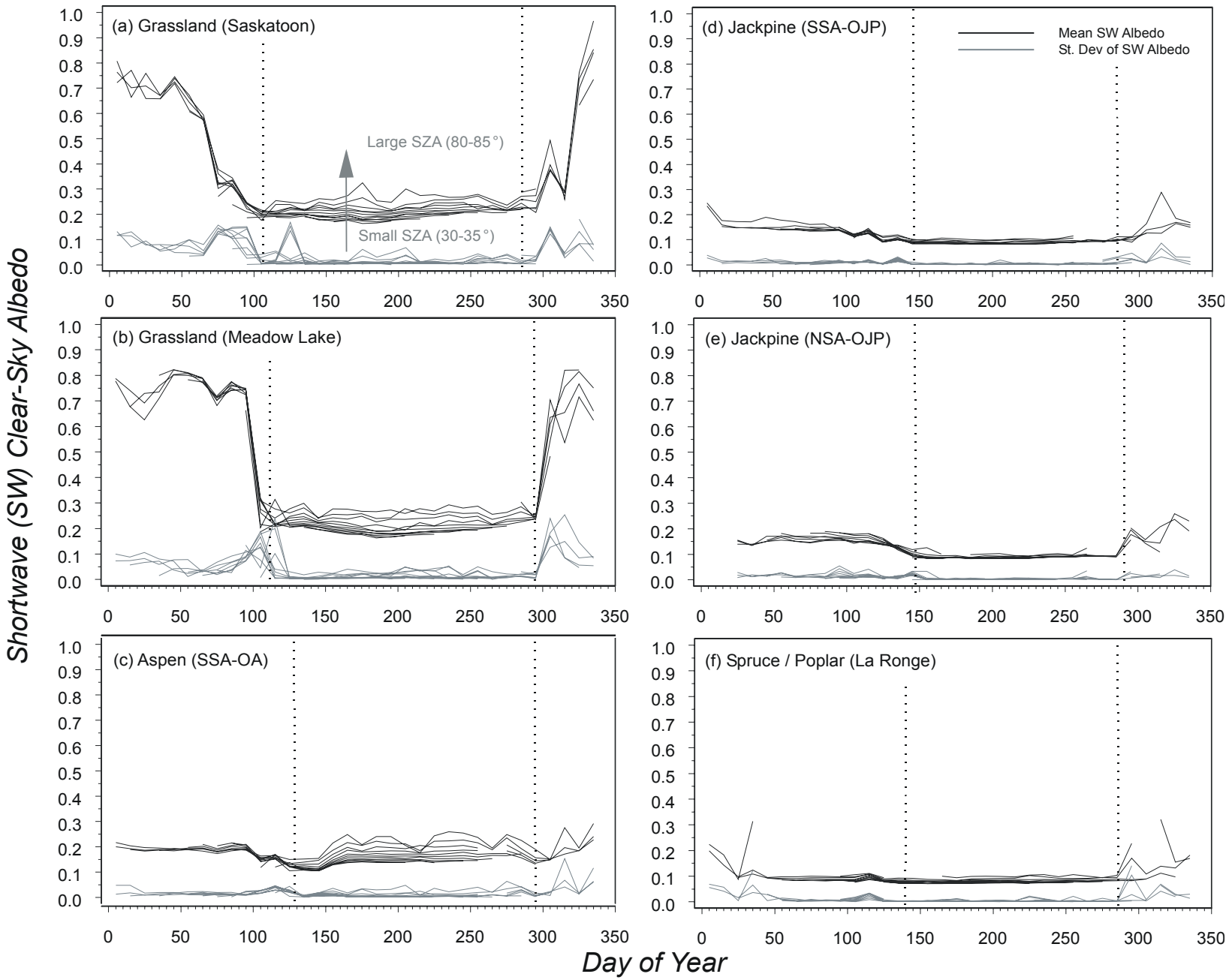

Figure 2. The temporal relationship between clear-sky shortwave albedo and solar zenith angle (SZA) for different land cover types as derived from AMS. Each point plotted represents the average albedo for a 7-day period in 1996. Each black line (-) corresponds to mean albedo values for 5° SZA intervals. Each grey line (-) corresponds to the standard deviations around these mean values. Vertical dashed lines separate snow-covered and snow-free periods.

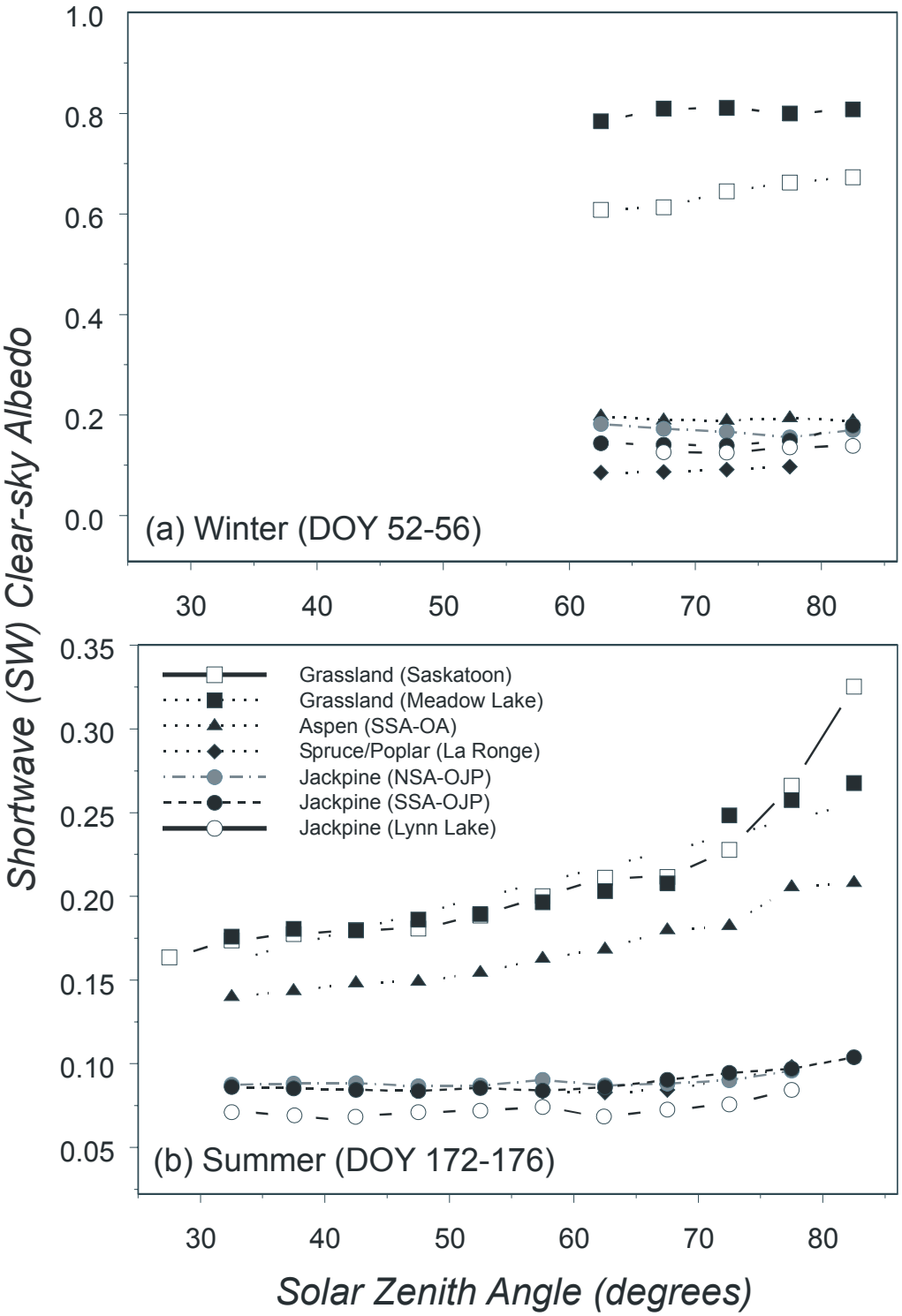

Figure 3. Diurnal relationships in surface albedo for different land cover types in winter (a) and summer (b) using AMS observations. Each point plotted represents the average shortwave clear-sky albedo for a consecutive 4-day period for grassland (□, ■), Broadleaf (▲), Needleleaf (○, ●, ●) and Mixed (◆) forest flux towers.

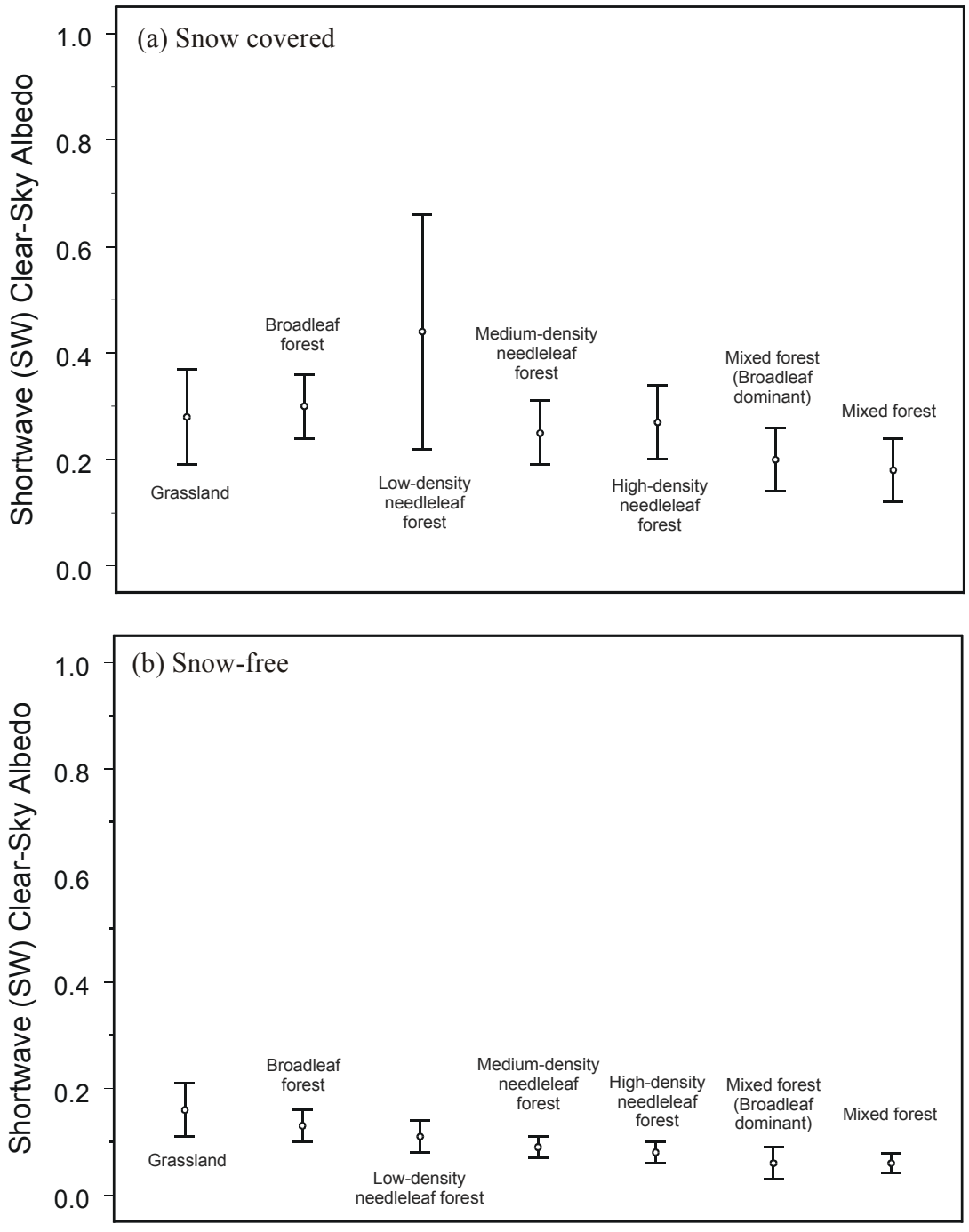

Figure 4. The relationship between land cover type and clear-sky albedo as derived from GOES-8 observations. Panels show the mean albedo of each vegetation type and its variability (standard deviation around mean) for surface conditions where snow is present (a) and absent (b).

Figure 5 shows the GOES-based temporal variations in albedo for snow-covered and snow-free periods over six cover types. This figure also shows the effects that solar zenith angle have on canopy albedo. Figure 5 reinforces the previously described differences in albedo between snow-covered and snow-free ground conditions. The influence of SZA on surface albedo varies with cover type and snow cover conditions. The influence of SZA on albedo is generally strongest where the ground is covered by snow. Under these conditions, the albedo of low-density needleleaf forest is most sensitive to changes in SZA (Figure 5(f)), while the albedo of mixed forest is least sensitive (Figure 5(c)). Where snow is absent, the albedos of grassland and broadleaf forest are most sensitive to changes in SZA (Figures 5(a) and (b)), while the albedos of all needleleaf forest types and mixed forest are less sensitive. The presence of snow also affects the variability in observed albedo for each cover type. In general, albedo observations are more variable where snow is present compared to where it is absent. This is especially true for low-density needleleaf forest.

Figure 6 provides an example of the diurnal relationships between albedo and SZA for winter and summer days. Figure 6 shows that the winter diurnal effects of SZA on albedo are less clear than those described for tower data. The effects of SZA on albedo are strongest for needleleaf forest in winter (Figure 6(a)) and strongest for grassland in summer (Figure 6(b)). Only weak SZA-albedo effects are observed for the other land cover types.

3.3 Comparison of Local- and Regional-scale data

Figure 7 illustrates the degree to which the tower-based albedo measurements correspond to those derived from GOES-8 observations. It shows the differences between tower- and GOES-based albedos for 7 of the land cover classes used in the regional-scale study (note: differences for the “mixed forest” and “mixed forest (broadleaf dominant)” types are both illustrated in panel (c)). Each plot contains a “line of equivalence”, $y = 0$, where tower-derived albedos are equal to regional-scale observations. Data plotted above this line represents periods when tower-based albedos provide too high estimates of regional-scale albedo. Data plotted below this line represent periods when tower-based albedos provide too low estimates of regional-scale albedo.

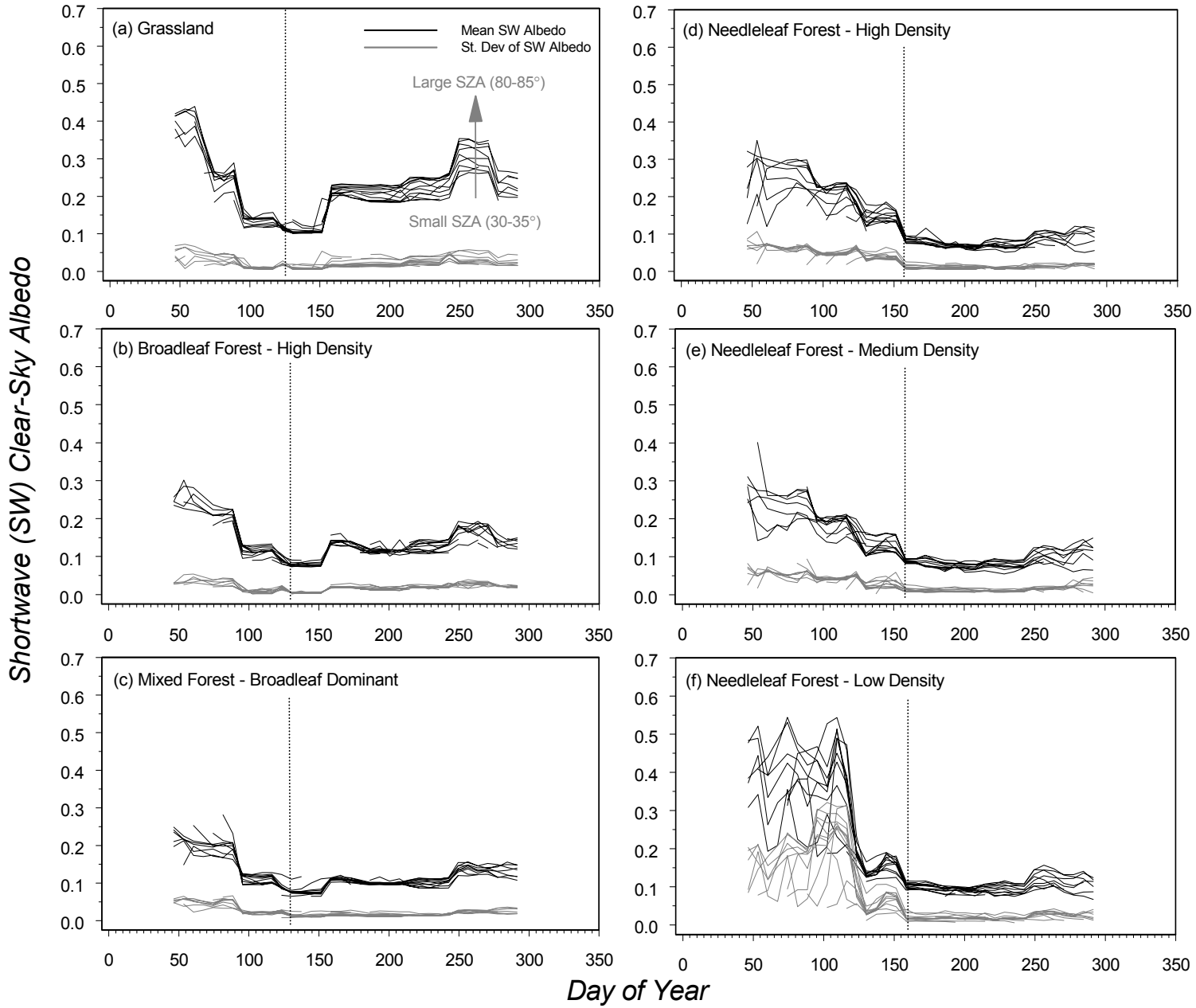

Figure 5. The temporal relationship between vegetation type, clear-sky shortwave albedo and solar zenith angle (SZA) as derived from GOES-8 measurements. Each point plotted represents the average albedo for a 7-day period in 1996. Each black line (**-**) corresponds to mean albedo values for 5° SZA intervals. Each grey line (-) corresponds to the standard deviations around these mean values. Vertical dashed lines separate snow-covered and snow-free periods.

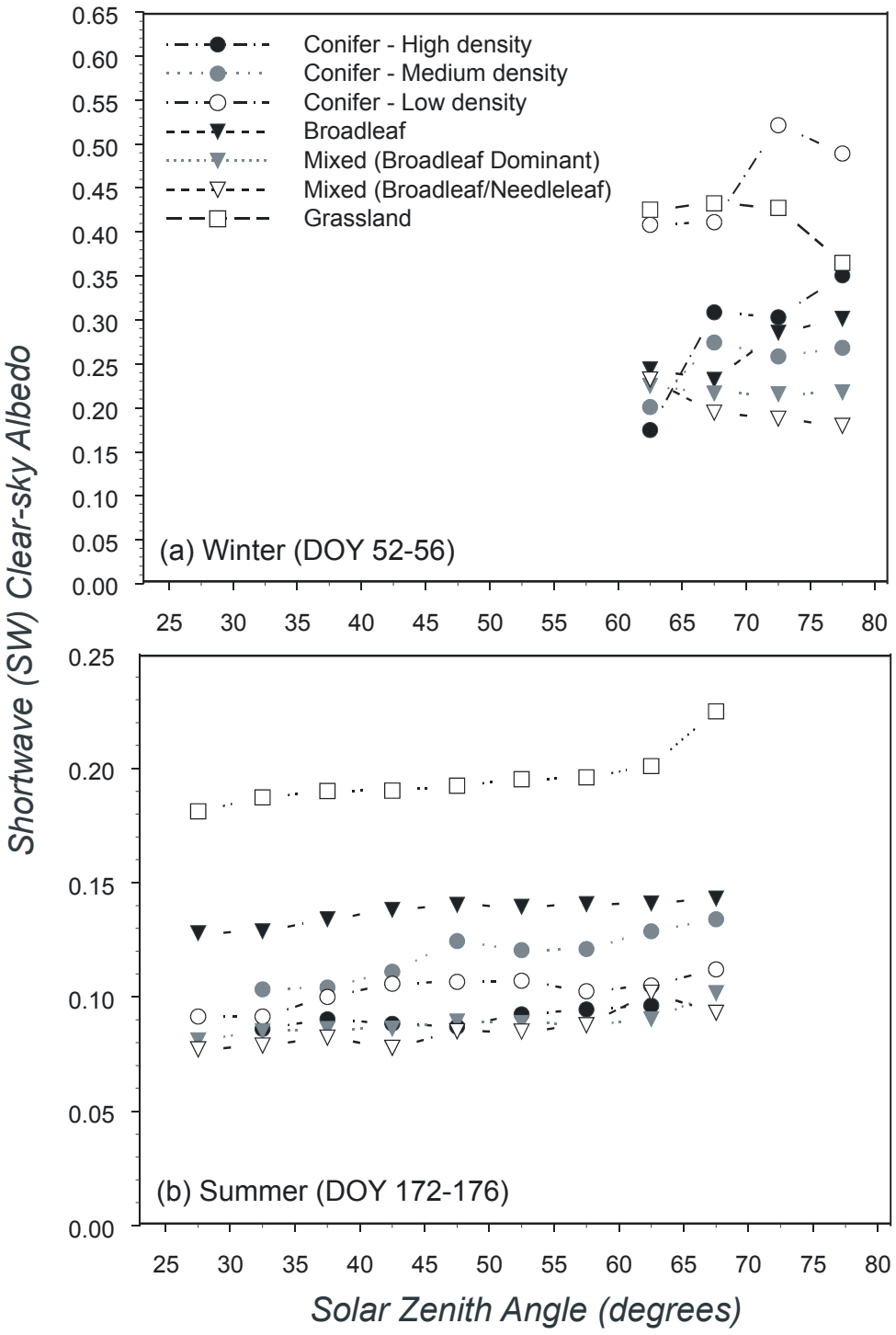

Figure 6. Diurnal relationships in surface albedo for different land cover types in winter (a) and summer (b) using GOES-8 observations. Each point plotted represents the average shortwave clear-sky albedo for a consecutive 4-day period for grassland (□), broadleaf forest (▼), mixed forest (▽, ▼), and needleleaf forest (○, ●, ●) cover types.

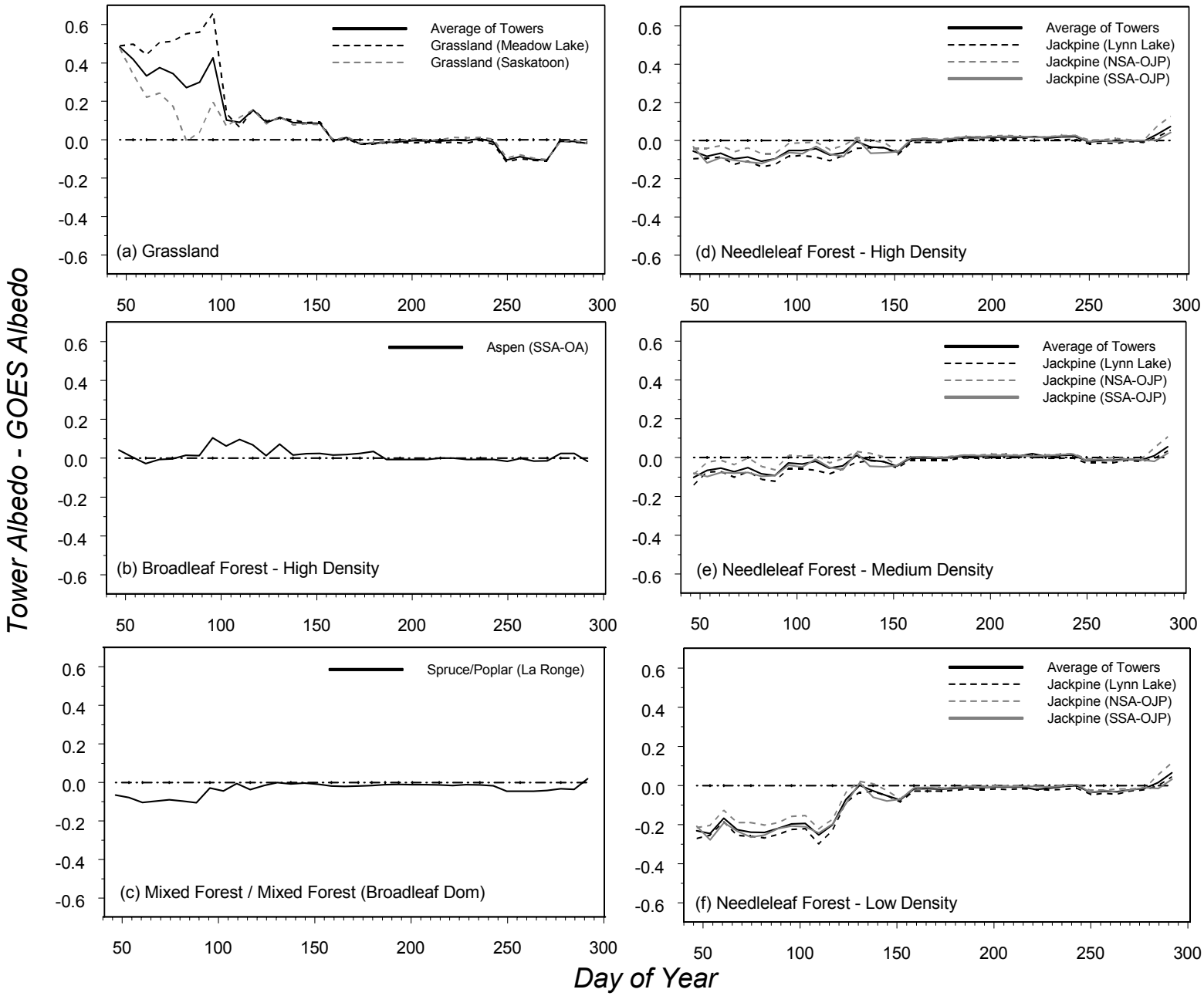

Figure 7. A comparison of tower- and GOES-based albedo observations through time. Panels show the absolute difference between GOES-8 observations and tower data for 7 of the land cover classes used in the regional-scale study. Albedo observations have been averaged for 7-day periods, and only use observations for SZA < 80°. Where more than one tower observation exists for a given cover type, we have also calculated the difference using the average of all towers. To aid in the interpretation of each panel, we have also included a "line of equivalence" which matches the line of no difference between the tower and GOES-8 observations. Note that we compare observations from the three Jackpine tower sites with the three different needleleaf land cover classes, and that the Spruce / Poplar tower data is compared with both the Mixed forest and Mixed forest (Broadleaf dominant) cover types in panel (c).

Figure 7 shows that the ability of tower data to characterize regional-scale albedo varies with season and cover type. The largest differences between the tower and GOES observations occur when the ground surface is covered by snow. This is especially the case for grassland (where observations from one of the towers are greater than regional-scale albedos by as much as 0.6), low-density needleleaf forest (where tower observations are lower than regional-scale albedos by as much as 0.3), and to a lesser extent, high- and medium-density needleleaf forest (where tower observations are lower than regional-scale albedos by as much as 0.15). In comparison, tower albedo observations are generally within 0.05 those of regional-scale observations during the growing season when the ground surface is snow-free. The exception to this trend occurs in late summer (DOY 240-280) for grassland, where tower sites are lower than regional-scale albedo by 0.12.

4. Discussion

4.1 Local-scale data

The results of the local-scale study highlight three important trends (Figures 1, 2 and 3). These are (a) that surface albedos progressively decrease as one moves from grassland to broadleaf forest, needleleaf forest, and mixed forest canopies, (b) that these albedos become less sensitive to changes in SZA as one moves through these environments, and (c) that the presence of snow on the ground not only increases the albedos of all cover types, but also increases their sensitivities to changes in SZA. These trends are generally consistent with the results of other studies.

The patterns of albedo among grassland, broadleaf forest, needleleaf forest and mixed forest are supported by the results of other *in situ* studies (e.g, Sellers et al., (1995) and Betts and Ball (1997), who used BOREAS tower data from 1994 and 1995). These studies showed similar relationships for surface conditions where snow was present and absent (Betts and Ball, 1997), as well as for both conditions combined (Sellers et al., 1995). The observed differences in albedo among cover types can be explained as follows. Canopy albedo is inversely correlated to various factors, including (a) the horizontal heterogeneity of canopy elements, (b) the degree of clumping of leaves or needles within individual plants, (c) the degree to which plant leaves or needles are

vertically oriented (Dickinson, 1983). Each of these factors decreases albedo by increasing the amount of incoming solar radiation that is trapped by the canopy. As a result, the albedo of grassland is significantly higher than that of forest canopies, and the albedo of broadleaf forest site is significantly higher than those of the needleleaf and mixed forest sites. The different structural characteristics of needleleaf and mixed forest tree species determine the albedos of their respective canopies. The needleleaf forest sites used in this study are dominated by Jackpine, while the mixed forest sites are dominated by Spruce and Poplar. The spire-shaped crowns of Spruce are more efficient at trapping incoming radiation than the rounded crowns of Jackpine. This, in addition to the added heterogeneity supplied by Poplar trees, makes the mixed forest site more structurally complex than the needleleaf forest sites. As a result, the albedos of mixed forest tend to be lower than those of needleleaf forest.

The effects of snow on the albedos of grassland, broadleaf forest, needleleaf forest and mixed forest are supported by the results of other *in situ* studies. In 1994, Betts and Ball (1997) explicitly studied the effects of snow on the albedo of the 10 BOREAS tower sites. Their results showed that the presence of snow increased grassland albedo by 0.547, broadleaf forest albedo by 0.098, needleleaf forest albedo by 0.065 and mixed forest albedo by 0.027. These increases are slightly larger (≈ 0.05) than the average increases calculated from the *in situ* data used in this study. The highly variable effects of snow on surface albedo illustrate the large impact of canopy shading on winter albedo values (Betts and Ball, 1997). The lack of taller plant forms at the grassland sites means that even small snowfalls can produce highly reflective surfaces. The effects of snow cover on the albedos of Aspen-dominated broadleaf forest occur because these canopies provide considerably less shadowing in winter when the canopy is not in leaf. In comparison, the effects of snow are least for the needleleaf and mixed sites whose year-round canopies provide the most shadowing. Canopy shadowing is the dominant mechanism controlling the influence of snow cover on surface albedo in the boreal region because the snow that is intercepted by the forest canopy is quickly removed by wind or through sublimation (Pomeroy et al., 1998; Gamon et al.).

The observed different effects of SZA on the albedos of grassland, broadleaf forest, needleleaf forest and mixed forest sites are supported by other *in situ* observations.

Sellers et al., (1995) used tower data to illustrate the overall dependencies of albedo on solar position. While the results of their study are consistent with those reported here, their study differed from ours in that it (a) failed to consider how the presence of snow affects these dependencies, and (b) ignored the influence of time of albedo-SZA relationships. Betts and Ball (1997) used tower data to calculate the mean albedos for each site under conditions where snow was present and absent. Their study did not explcitly investigate the effects of SZA on albedo, but the standard deviations associated with their albedo values are consistent with the results provided here. The observed dependencies of albedo on SZA can be explained as follows. The sensitivity of albedo to changes in solar zenith angle is largely determined by the heterogeneity of the surface cover (Sellers et al., 1995). Heterogeneous canopies, such as forests, are less sensitive to changes in SZA than homogeneous canopies, such as grassland. This is because rougher canopies have less diurnal variation due to increased shadowing by vertical roughness elements as SZA increases (Dickinson, 1983). The crown shapes of Jackpine and Spruce cause more shadowing to occur in needleleaf forest compared to the Aspen-dominated broadleaf forest. As a result, the needleleaf and mixed forest canopies show very little changes in albedo from low to high SZAs, compared to broadleaf forest and grassland. Our results also suggest that the presence of snow makes canopies more sensitive to changes in SZA.

4.2 Regional-scale data

The results of the regional-scale study highlight three important trends (see Figures 5, 6 and 7). These are (a) that surface albedos progressively decrease as one moves from grassland to broadleaf forest, needleleaf forest, and mixed forest environments (although the albedos of needleleaf and mixed forests are similar when snow is absent), (b) that the albedo of grassland is most sensitive to changes in SZA, while the albedos of needleleaf and mixed forests are least sensitive to changes in SZA, and (c) that the presence of snow on the ground not only increases the albedo of all cover types, but also their sensitivities to changes in SZA.

The GOES-derived mean regional albedos of needleleaf, broadleaf and mixed forest canopies are consistent with the snow-covered and snow-free MODIS albedos

described by Jin et al., (2002). While our regional albedo estimates over snow-free grassland are also consistent with these observations, they are considerably lower (≈ 0.25) than the MODIS albedos over snow-covered grassland. However, it is important to note that the results of these studies are not strictly comparable because Jin et al (2002) used finer-resolution albedo data (1km), and a more general land cover classification scheme (IGBP), than those used in our study.

The observed three trends are generally consistent with the patterns of albedo among the various cover types used in our tower-based study, despite being derived for a much coarser spatial resolution. Our results, and the decreasing albedos as one moves from low- to medium- to high-density needleleaf forest suggest that the various shadow-causing canopy mechanisms described previously also combine to control surface albedo at a regional scale. The extremely high albedo of low-density needleleaf forest in winter is likely due to a combination of two factors. First, low stem density means that less within-canopy shadowing occurs compared to higher density forests. This allows a higher exposure of underlying snow cover in low-density forests. Second, the understory of this forest type commonly comprises highly reflective frozen wetlands and water bodies that are largely absent from the other forest types. The low albedos of grassland are surprising and need to be further investigated.

4.3 Comparison of Local- and Regional-scale data

The direct comparison of local- and regional-scale albedos (Figure 7) shows that the tower sites generally provide a reasonable characterization of regional-scale albedo when the ground surface is snow-free, but an often-poor characterization of surface albedo (> 0.15) when snow is present. Where snow is absent, these absolute errors correspond to relative errors of 5-20% for grassland and broadleaf forest, and 10-15% for high-, medium- and low-density needleleaf forest. Where snow is present, relative errors are as high as 30% for medium-density needleleaf forest, 50% for high-density needleleaf forest, 75% for low-density needleleaf forest, 80% for broadleaf and mixed forest, and 450% for grassland. The difference between *in situ* albedo observations and the regional albedo estimates of mixed and needleleaf forest canopies in winter are consistent with the results of Jin et al., (2002), who noted that satellites may see a larger fraction of sunlit

gaps between forest stands compared to tower observations, and hence, provide larger estimates of albedo. The disparity between *in situ* albedo observations and those collected over low-density needleleaf forest are particularly a concern because this cover type comprises 18% of the BOREAS study area, and its mis-specification in climate models could lead to large errors in energy balance across the boreal region. The differences between *in situ* and GOES observations over grassland are also consistent with the results of Jin et al., (2002). These differences are likely caused by the considerably different spatial resolutions of these data sets. The surface heterogeneity in grasslands causes less broken snow at smaller scales. As a result, *in situ* observations are more likely to include the high albedos typical of flat and completely snow-covered areas (i.e. "pure" snow albedos). In comparison, GOES albedo observations over snow-covered grassland are likely to be influenced by other factors, such as snow-free ground, shadowing by snowdrifts, and/or dirty or large crystal snow surfaces (Jin et al, 2002). However, the larger disparity between *in situ* and GOES observations over grassland is less important in this study because grassland only comprises 1% of the total study area.

4.4 Limitations of study and other considerations

Although the above results have large implications for those wishing to characterize regional-scale surface albedo using *in situ* observations, our study is limited on several counts. First, we have restricted our study to clear-sky albedo. However, the effects of scale, snow and SZA on albedo may be different under cloudy sky conditions. Any further study of the correspondence between *in situ* and regional-scale albedos should explicitly consider this. Second, although our screening of *in situ* observations was designed to exclude "bad" data, it is inevitable that spurious observations were included in our analyses. However, our screening criteria were conservative, and thus we are relatively confident that such errors are small. Third, while the use of training areas in our regional-scale study was designed to exclude albedo observations that were influenced by more than one cover class, it is inevitable that mixed-class spectra will influence the above results. Fourth, our methods of separating the albedo characteristics of snow-covered and snow-free conditions are limited in two ways. At the local scale, the criterion used to define snow-covered ground (snow depth > 0mm) is too liberal. This is

because albedo measurements may also be influenced by the albedos of snow-free surfaces under very low snow depths. Low snow depths may also correspond to times of the year when meltwater accumulates on the snow surface, lowering measured albedo and further biasing results. Thus, future studies should use higher thresholds for defining snow-covered ground. At the regional scale, the snow dataset utilized was at a much coarser spatial resolution than our albedo data (25km and 4km, respectively). Thus, our calculated albedos for snow-covered and snow-free surfaces will include unknown errors of omission and commission. However, because we excluded periods of highly variable snow cover from these analyses, spurious observations likely comprise only a tiny percentage of the total pixels used. Fifth, we have limited our validation of albedo-SZA relationships to relationships derived from other field measurements (Sellers et al., 1995; Betts and Ball, 1997) and to theory (Dickinson, 1983). However, there have also been many attempts to characterize the bidirectional reflectance distribution function (BRDF) of vegetated surfaces, from which albedo-SZA relationships can be extracted. These include mathematical modelling approaches (e.g. Nilson and Kuusk, 1989), and approaches using spectral observations from *in situ* (Abdou et al., 2000), airborne (e.g. Ranson et al., 1994; Schaaf and Strahler, 1994; Leblanc et al., 1999) and spaceborne (e.g. MODIS and MISR: Wanner et al., 1997; Lucht et al., 2000a; Schaaf et al., 2002; Jin et al., 2003a; Jin et al., 2003b) sensors. Further comparisons of *in situ* and satellite-derived albedo-SZA relationships should also consider such studies. Sixth, our comparison of *in situ* and regional-scale albedos were carried out using data aggregated to a weekly time scale. We made no attempt to compare the correspondence of these data at finer temporal resolutions (eg days; hours). Further comparisons of *in situ* and satellite-derived albedos should address this issue.

5. Conclusions

The work presented here analyzes and compare the local- and regional-scale albedo characteristics of the dominant land cover types found within the North American boreal region, assesses the the effects of snow cover on these characteristics, and quantifies the potential bias that can result from using local-scale observations to describe surface albedos across larger geographical extents. We have used *in situ* and satellite albedo data

to show (a) that the patterns of albedo among land cover types are consistent at both local and regional scales, (b) that the albedos of grassland and broadleaf canopies are most sensitive to changes in SZA, while the albedos of needleleaf forest and mixed canopies are less sensitive to changes in SZA, (c) that snow cover not only increases the albedo of all cover types, but also increases their sensitivities to changes in SZA, and (d) that weekly-averaged *in situ* observations provide a reasonable characterization of regional-scale albedo when the ground is snow-free, but an often-poor characterization when snow is present. The patterns of albedo among the land cover types considered here – and the sensitivity of these types to changes in SZA – are consistent with other studies, and are caused by various canopy properties that influence within-canopy shadowing.

The implications of our results include (a) that weekly-averaged *in situ* measurements provide reasonable estimates of surface albedo on a regional-scale over snow-free surfaces, but can lead to large absolute and relative errors in albedo where snow is present, (b) that these errors are particularly a concern for low-density needleleaf forest because it covers 18% of the BOREAS study area, and its mis-specification in climate models could lead to large errors in energy balance across the boreal region, and (c) that forest canopy density is an important factor influencing the agreement between *in situ* and regional-scale observations where snow is present, but is unimportant when snow is absent. Further attempts to compare *in situ* and regional-scale albedos should focus their attentions on reducing the disparity between data, especially over snow-covered surfaces. Such studies should also consider the effects of other components of albedo (i.e. albedo under cloudy conditions), as well as finer time scales (eg days; hours). We are currently refining our approach in response to these issues.

6. Acknowledgements

We gratefully thank A.K. Betts, J. Gu and J. Nickeson for their advice on data and its processing. This work was funded by the Canadian Climate Change Action Fund (CCAF).

7. References

Abdou, W.A., Helmlinger, M.C., Conel, J.E., Bruegge, C.J., Pilorz, S.H., Martonchik, J.V., and Gaitley, B.J. (2000), Ground measurements of surface BRF and HDRF using PARABOLA III. *Journal of Geophysical Research*, 106(D11), 11967-11976.

Armstrong, R.L., and Brodzik, M.J. (2002). Northern Hemisphere EASE-Grid weekly snow cover and sea ice extent Version 2 [CD-ROM]. National Snow and Ice Data Center, Boulder, Colorado, USA. [http://www-nsidc.colorado.edu/data/nsidc-0046.html]

Betts, A.K., and Ball, J.H. (1997), Albedo over the Boreal forest. *Journal of Geophysical Research*, 102(D24), 28901-28909.

Betts, R.A. (2000), Offset of the potential carbon sink from boreal forestation by decreases in surface albedo. *Nature*, 408, 187 - 190.

Bonan, G.B., Pollard, D., and Thompson, S.L. (1992), Effects of boreal forest vegetation on global climate. *Nature*, 359, 716-718.

Cao, C., and Siu-Ngan Lam, N. (1997) Understanding the scale and resolution effects in Remote Sensing and GIS. In Quattrochi, D.A., and Goodchild, M.F. (eds). CRC Press, Boca Raton, Florida, USA, pp. 57-72.

Chen, J.M., Rich, P.M., Gower, S.T., Norman, J.M., and Plummer, S. (1997), Leaf area index of boreal forests: Theory, techniques and measurements. *Journal of Geophysical Research*, 102(D24), 29429-29443.

Cihlar, J., Beaubien, R., Latifovic, R., and Simard, G. (1999) Land Cover of Canada version 1.1. In *Special Publication, NBIOME Project*. Ottawa, Ontario, Canada.: Produced by the Canada Centre for Remote Sensing and the Canadian Forest Service, Natural Resources Canada.

Cornwall, C., Horiuchi, A., and Lehman, C. (2003). NOAA Solar Position Calculator. [http://www.srrb.noaa.gov/highlights/sunrise/solareqns.PDF]

Dickinson, R.E. (1983), Land surface processes and climate-surface albedos and energy balance. *Advances in Geophysics*, 25, 305-353.

Gamon, J.A., Huemmrich, K.F., Peddle, D.R., Chen, J., Fuentes, D., Hall, F.G., Kimball, J.S., Goetz, S., Gu, J., and McDonald, K.C. (2004), Remote sensing in BOREAS: Lessons learned. *Remote Sensing of Environment*, 89, 139-162.

Gu, J., and Smith, E.A. (1997), High-resolution estimates of total solar and PAR surface fluxes over large-scale BOREAS study area from GOES measurements. *Journal of Geophysical Research*, 102(D24), 29685-29705.

Gu, J., Smith, E.A., and Merritt, J.D. (1999), Testing energy balance closure with GOES-retrieved net radiation and in situ measured eddy correlation fluxes. *Journal of Geophysical Research*, 104(D22), 27881-27893.

Gu, J., Smith, E.A., Hodges, G., and Cooper, H.J. (1997), Retrieval of daytime surface net longwave flux over BOREAS from GOES estimates of surface solar flux and surface temperature. *Canadian Journal of Remote Sensing*, 23(2), 176-187.

Henderson-Sellers, A., and Wilson, M.F. (1983), Surface albedo data for climatic modeling. *Reviews of Geophysics*, 21, 1743-1778.

IPCC (2001) Summary for policy makers. In: A report of working group I of the intergovernmental panel on climate change.

Jin, Y., Schaaf, C.B., Gao, F., Li, X., Strahler, A.H., Lucht, W., and Liang, S. (2003a), Consistency of MODIS surface bidirectional reflectance distribution function and albedo retrievals: 1. Algorithm Performance. *Journal of Geophysical Research*, 108(D5).

Jin, Y., Schaaf, C.B., Gao, F., Li, X., Strahler, A.H., Lucht, W., Zeng, X., and Dickinson, R.E. (2002), How does snow impact the albedo of vegetated land surfaces as analyzed with MODIS data? *Geophysical Research Letters*, 29(10).

Jin, Y., Schaaf, C.B., Woodcock, C.E., Gao, F., Li, X., Strahler, A.H., Lucht, W., and Liang, S. (2003b), Consistency of MODIS surface bidirectional reflectance distribution function and albedo retrievals: 2. Validation. *Journal of Geophysical Research*, 108(D5).

Knapp, D., and Newcomer, J. (1999) BOREAS Derived Surface Meteorological Data. Collected Data of The Boreal Ecosystem-Atmosphere Study. National Aeronautics and Space Administration , Goddard Space Flight Center, Greenbelt, Maryland, U.S.A. CD-ROM. Available from Oak Ridge National Laboratory Distributed Active Archive Center, Oak Ridge, Tennessee, U.S.A. [http://www.daac.ornl.gov].

Leblanc, S.G., Bicheron, P., Chen, J.M., Leroy, M., and J., C. (1999), Investigation of directional reflectance in boreal forests using an improved 4-Scale model and

airborne POLDER data. *IEEE Transactions on Geoscience and Remote Sensing*, 37(3), 1396-1414.

Li, Z., and Garand, L. (1994), Estimation of surface albedo from space: A parameterization for global application. *Journal of Geophysical Research*, 99(D4), 8335-8350.

Liang, S., Shuey, C.J., Russ, A.L., Fang, H., Chen, M., Walthall, C.L., Daughtry, C.S.T., and Hunt Jr., R. (2002a), Narrowband to broadband conversions of land surface albedo: II. Validation. *Remote Sensing of Environment*, 84, 25-41.

Liang, S., Fang, H., Chen, M., Shuey, C.J., Walthall, C., Daughtry, C., Morisette, J., Schaaf, C., and Strahler, A. (2002b), Validating MODIS land surface reflectance and albedo products: methods and preliminary results. *Remote Sensing of Environment*, 83(1-2), 149-162.

Lucht, W., Schaaf, C.B., and Strahler, A.H. (2000a), An algorithm for the retrieval of albedo from space using semiempirical BRDF models. *IEEE Transactions on Geoscience and Remote Sensing*, 38(2), 977-998.

Lucht, W., Hyman, A.H., Strahler, A.H., Barnsley, M.J., Hobson, P., and Muller, J.-P. (2000b), A comparison of satellite-serived spectral albedos to ground-based broadband albedo measurements modeled to satellite spatial scale for a semidesert landscape. *Remote Sensing of Environment*, 74, 85-98.

Newcomer, J., Landis, D., Conrad, S., Curd, S., Huemmrich, K., Knapp, D., Morrell, A., Nickeson, J., Papagno, A., Rinker, D., Strub, R., Twine, T., Hall, F., and Sellers, P. (2000) Collected Data of The Boreal Ecosystem-Atmosphere Study. National Aeronautics and Space Administration, Goddard Space Flight Center, Greenbelt, Maryland, U.S.A. CD-ROM. Available from Oak Ridge National Laboratory Distributed Active Archive Center, Oak Ridge, Tennessee, U.S.A. [http://www.daac.ornl.gov].

Nickeson, J., Landis, D., and Hall, F. (2002) Collected Data of The Boreal Ecosystem-Atmosphere Study Follow-On. NASA. National Aeronautics and Space Administration, Goddard Space Flight Center, Greenbelt, Maryland, U.S.A. CD-ROM. Available from Oak Ridge National Laboratory Distributed Active Archive Center, Oak Ridge, Tennessee, U.S.A. [http://www.daac.ornl.gov].

Nilson, T., and Kuusk, A. (1989), A reflectance model for the homogeneous plant canopy and its inversion. *Remote Sensing of Environment*, 27(2), 157-167.

Pinty, B., and Verstraete, M. (1992), On the design and validation of surface bidirectional reflectance and albedo model. *Remote Sensing of Environment*, 41, 155-167.

Pomeroy, J.W., Parviainien, J., Hedstrom, N., and Gray, D.M. (1998), Coupled modeling of forest snow interception and sublimation. *Hydrological Processes*, 12, 2317-2337.

Ranson, K.J., Irons, J.R., and Williams, D.L. (1994), Multispectral bidirectional reflectance of northern forest canopies with the Advanced Solid-State Array Spectroradiometer (ASAS). *Remote Sensing of Environment*, 47, 276-289.

Rowe, C.M. (1991), Modeling land-surface albedos from vegetation canopy architecture. *Physical Geography*, 12(2), 93-114.

Schaaf, C.B., and Strahler, A.H. (1994), Validation of bidirectional and hemispherical reflectances from a geometric-optical model using ASAS imagery and pyranometer measurements of a spruce forest. *Remote Sensing of Environment*, 49(2), 138-144.

Schaaf, C.B., Gao, F., Strahler, A.H., Lucht, W., Li, X., Tsang, T., Strugnell, N.C., Zhang, X., Jin, Y., and Muller, J.-P. (2002), First operational BRDF, albedo nadir reflectance products from MODIS. *Remote Sensing of Environment*, 83(1-2), 135-148.

Sellers, P.J., Hall, F.G., Margolis, H., Kelly, B., Baldocchi, D., den Hartog, G., Cihlar, J., Ryan, M.G., Goodison, B., Crill, P., Ranson, K.J., Lettenmaier, D., and Wickland, E. (1995), The Boreal Ecosystem-Atmosphere Study (BOREAS): An Overview and Early Results from the 1994 Field year. *Bulletin of the American Meteorological Society*, 76(9), 1549-1577.

Sellers, P.J., Hall, F.G., Kelly, B., Black, A., Baldocchi, D., Berry, J.A., Ryan, M., Ranson, K.J., Crill, P., Lettenmaier, D., Margolis, H., Cihlar, J., Newcomer, J., Fitzjarrald, D., Jarvis, P.G., Gower, S.T., Halliwell, D., Williams, D., Goodison, B., Wickland, E., and Guertin, F.E. (1997), BOREAS in 1997: Experiment overview, scientific results and future directions. *Journal of Geophysical Research*, 102(D24), 28731-28769.

Shewchuk, S.R. (2000) Atmospheric Sciences Infrastructure Core Measurements for BOREAS (AFM-07). In Newcomer, J., Landis, D., Conrad, S., Curd, S., Huemmrich, K., Knapp, D. et al. (eds), Collected Data of The Boreal Ecosystem-Atmosphere Study. National Aeronautics and Space Administration, Goddard Space Flight Center, Greenbelt, Maryland, U.S.A. CD-ROM. Available from Oak Ridge National Laboratory Distributed Active Archive Center, Oak Ridge, Tennessee, U.S.A. [http://www.daac.ornl.gov].

Smith, E.A., Gu, J., and Nickeson, J. (2001) BOREAS Follow-On HMet-01 Level-2 GOES-8 1996 Shortwave and Longwave Radiation. Collected Data of The Boreal Ecosystem-Atmosphere Study. National Aeronautics and Space Administration, Goddard Space Flight Center, Greenbelt, Maryland, U.S.A. CD-ROM. Available from Oak Ridge National Laboratory Distributed Active Archive Center, Oak Ridge, Tennessee, U.S.A. [http://www.daac.ornl.gov].

Song, J., and Gao, W. (1999), An improved method to derive surface albedo from narrowband AVHRR satelite data: narrowband to broadband conversion. *Journal of Applied Meteorology*, 38, 239-249.

Vikhamar, D., and Solberg, R. (2003), Subpixel mapping of snow cover in forests by optical remote sensing. *Remote Sensing of Environment*, 84(1 SU -), 69-82.

Wang, S., Chen, W., and Cihlar, J. (2002), New calculation methods of diurnal distributions of solar radiation and its interception by canopy over complex terrain. *Ecological Modelling*, 155, 191-204.

Wanner, W., Strahler, A.H., Hu, B., Lewis, P., Muller, J.-P., Li, X., Schaaf, C.B., and Barnsley, M.J. (1997), Global retrieval of bidirectional reflectance and albedo over land from EOS MODIS and MISR data: Theory and algorithm. *Journal of Geophysical Research*, 102, 17143-17161.

Yang, P.C., Black, T.A., Neumann, H.H., Novak, M.D., and Blanken, P.D. (1999), Spatial and temporal variability in CO2 concentration and flux in a boreal Aspen forest. *Journal of Geophysical Research*, 104(D22), 27653-27661.